AGU ADVANCING EARTH AND SPACE SCIENCE

JGR Oceans

RESEARCH ARTICLE

10.1029/2021JC017738

Key Points:

- In the Chukchi marginal area (CMA), aragonite saturation state (Ω_{arag}) at the surface was determined mainly by the mixing of seawater and fresh water
- In the East Siberian marginal area, Ω_{arag} was affected by freshwater mixing, biological production, and lateral mixing
- In the near future, most of surface waters in the CMA will be undersaturated with respect to aragonite

Correspondence to:

D. Kim,
dkim@kiost.ac.kr

Citation:

Kim, D., Yang, E.-J., Cho, S., Kim, H.-J., Cho, K.-H., Jung, J., & Kang, S.-H. (2021). Spatial and temporal variations of aragonite saturation states in the surface waters of the western Arctic Ocean. *Journal of Geophysical Research: Oceans*, *126*, e2021JC017738. https://doi.org/10.1029/2021JC017738

Received 12 JUL 2021
Accepted 19 OCT 2021

Author Contributions:

Conceptualization: D. Kim, E.-J. Yang
Data curation: S. Cho, H.-J. Kim
Formal analysis: D. Kim, S. Cho, K.-H. Cho, J. Jung
Investigation: H.-J. Kim, K.-H. Cho
Methodology: S. Cho, H.-J. Kim
Project Administration: E.-J. Yang, J. Jung
Resources: E.-J. Yang, J. Jung
Writing – original draft: D. Kim

Spatial and Temporal Variations of Aragonite Saturation States in the Surface Waters of the Western Arctic Ocean

D. Kim[1], E.-J. Yang[2], S. Cho[1], H.-J. Kim[1], K.-H. Cho[2], J. Jung[2], and S.-H. Kang[2]

[1]Marine Environmental Research Center, Korea Institute of Ocean Science & Technology, Busan, South Korea,
[2]Division of Polar Ocean Science, Korea Polar Research Institute, Incheon, South Korea

Abstract The aragonite saturation state (Ω_{arag}) was determined for the surface waters of the western Arctic Ocean over 3 years, from 2016 to 2018, in an investigation of the present state of acidification of its waters and the main factors controlling the spatial and temporal variations in the surface Ω_{arag}. The study area was divided into the Chukchi marginal area (CMA) and the East Siberian marginal area (ESMA) along a longitude of 180°E. In the CMA, the surface Ω_{arag} during the study period ranged from 0.86 to 1.77, with an average of 1.16, indicating near saturation with respect to aragonite. In the ESMA, the surface Ω_{arag} during the study period ranged from 1.01 to 2.21, with a higher average (1.59) than the CMA. Aragonite undersaturation in the ESMA was not observed during any of the measurement periods, so ocean acidification was less serious there than in the CMA. The surface Ω_{arag} of the CMA was mainly determined by the mixing of seawater and freshwater introduced from rivers and/or sea ice, whereas in the ESMA it was influenced by the mixing of seawater and freshwater but also biological production and lateral mixing.

Plain Language Summary The study was conducted in the western Arctic Ocean and included the Northwind Ridge, Chukchi Plateau, Chukchi Abyssal Plain, Chukchi Sea Slope, East Siberian Sea Slope, and Mendeleyev Ridge. The waters encompassed by these sites are highly vulnerable to acidification because of the inflow of lower-pH water from the Pacific Ocean through the Bering Sea and the current rapid reduction in the amount of sea ice. The study area was divided into the Chukchi marginal area (CMA) and the East Siberian marginal area (ESMA) along a longitude of 180°E. In the CMA, the surface waters were almost saturated with respect to aragonite but in the ESMA they were undersaturated, indicating that oceanic acidification was more serious in the CMA than in the ESMA. In the near future, the aragonite undersaturation in the most of the surface waters of the CMA will prohibit the survival of calcareous organisms and may lead to their extinction from this area. However, a similar short-term scenario is not expected in the ESMA, due to its relatively high biological production, which favors aragonite saturation and will thus delay aragonite undersaturation of the surface water.

1. Introduction

The Arctic Ocean is currently undergoing rapid environmental change, with a decline in the summer extent of sea ice of >40% since 1979 (Comiso et al., 2008) and further decreases over the next few decades predicted (Overland & Wang, 2013). Other changes, including increases in the sea surface temperature (SST; Steele et al., 2010), the freshening of surface waters (Timmermans et al., 2011), and increases in oceanic fluxes from the Pacific to the Arctic (Woodgate et al., 2012), have also been reported and have been attributed to global warming and climate change. Because sea ice limits air-sea gas exchange, its disappearance in summer enhances CO_2 exchange between the ocean and the atmosphere. In the Arctic Ocean, the surface partial pressure of CO_2 (pCO_2) is below the atmospheric level because of intense cooling, mixing with freshwater, and photosynthesis in summer (Bates et al., 2006; Gao et al., 2012). The increase in CO_2 uptake caused by the ice-free conditions decreases the pH of the surface waters. The enhanced uptake of CO_2 by seawater has decreased the pH values and the saturation state of calcium carbonate, a process known as ocean acidification (Orr et al., 2005).

Models of the Arctic Ocean also predict that the decrease in calcium carbonate saturation resulting from water freshening and the enhanced absorption of atmospheric CO_2 caused by sea ice melting will lead to an undersaturation of aragonite in Arctic surface waters within the next decade (Steinacher et al., 2009;

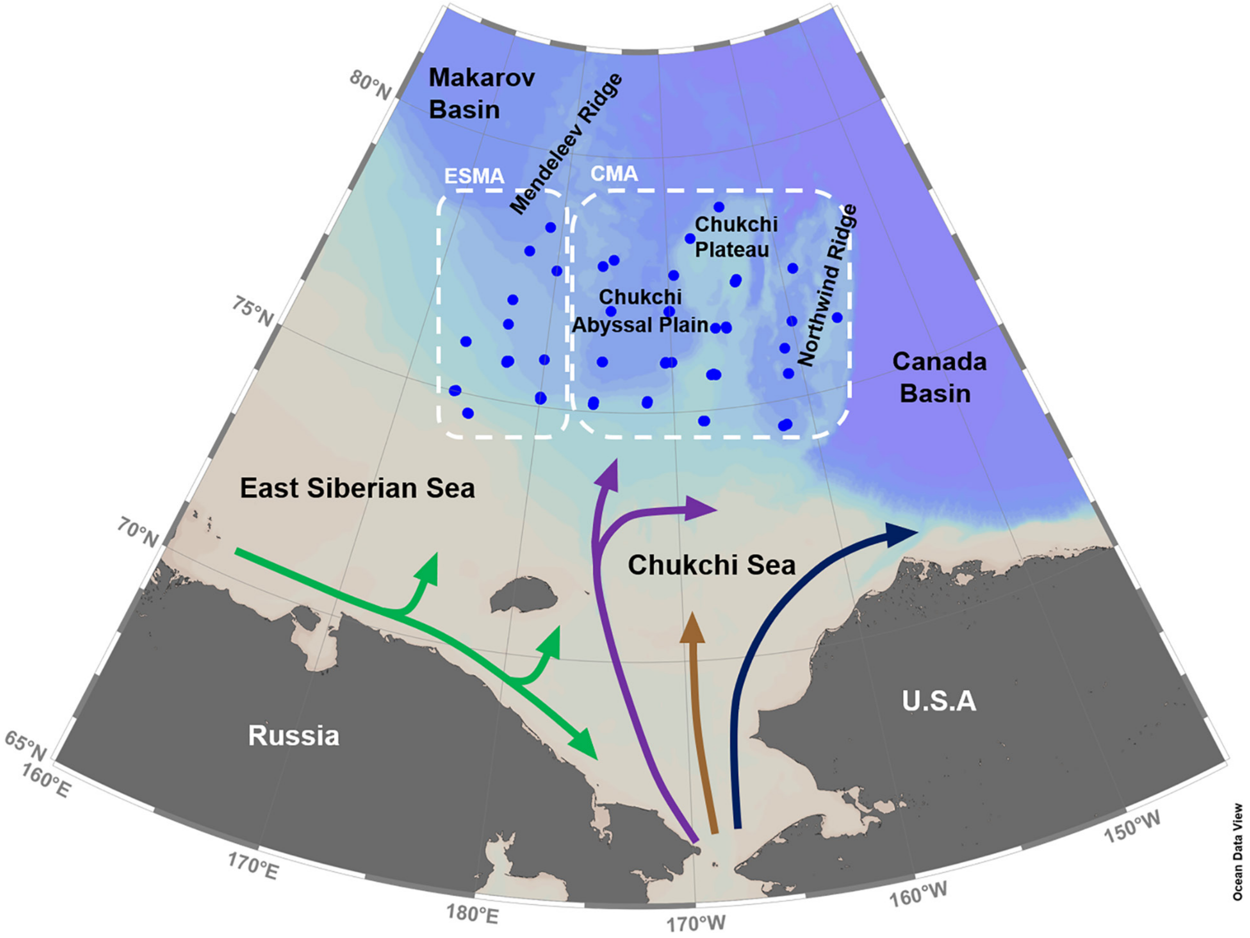

Figure 1. Map showing the sampling stations (blue dots) from 2016 to 2018 and the surface ocean circulation patterns. CMA implies the Chukchi marginal area, and ESMA is the East Siberian marginal area. The black line indicates Alaska coastal water, the brown line Bering Sea shelf water, the purple line Anadyr water, and the green line the Siberian coastal current (after Bai et al., 2019).

Yamamoto et al., 2012). Chierici and Fransson (2009) were the first to report the undersaturation of Arctic surface waters with aragonite, based on studies of the Canadian Arctic Archipelago and the Mackenzie Shelf in the summer of 2005. Similar findings were obtained in the Canada Basin of the Arctic Ocean in 2008 (Yamamoto-Kawai et al., 2009). Shortly thereafter, in a 2011 study, Robbins et al. (2013) estimated that ~20% of the basin's surface waters were undersaturated with aragonite. Most of the surface waters of the East Siberian and Laptev Seas were also found to be undersaturated, on the basis of data collected from 1999 to 2011 (Semiletov et al., 2016). However, the spatial extent of the undersaturated surface waters of the western Arctic Ocean has not been determined.

The focus of our study area was therefore the western Arctic Ocean, including the Northwind Ridge, Chukchi Plateau, Chukchi Abyssal Plain, Chukchi Sea Slope, East Siberian Sea Slope, and Mendeleyev Ridge (Figure 1). These waters are highly vulnerable to acidification because of the inflow of lower-pH water from the Pacific Ocean through the Bering Sea and the rapid melting of sea ice. Research on the carbonate chemistry of seawater in association with ocean acidification has mostly been performed in the Canada Basin and the continental shelves of the Chukchi and East Siberian Seas (Bates & Mathis, 2009; Bates et al., 2013; Cross et al., 2018; Mathis & Questel, 2013; Qi et al., 2017; Robbins et al., 2013; Semiletov et al., 2016; Yamamoto-Kawai et al., 2009, 2016), whereas the sites included in this study have largely been ignored. We determined the spatial extent of aragonite saturation (Ω_{arag}) in their surface waters over 3 years, from 2016 to 2018, to assess the present state of ocean acidification in the western Arctic Ocean. Interactions between seawater carbonate chemistry and physical and biogeochemical processes were also investigated, to identify the main factors controlling the spatial and temporal variations of the surface Ω_{arag} in the western Arctic Ocean.

2. Methods and Materials

2.1. Study Area

The study area is located in the western Arctic Ocean (74.5°N–78.0°N and 173.6°E–160.0°W), where water depths range from 90 to 2,210 m and the topography ranges from continental slope to deep basin (Figure 1). Along a longitude of 180°E, an eastern area was selected to include the Northwind Ridge, Chukchi Plateau, Chukchi Abyssal Plain, and Chukchi Sea Slope and a western area was selected to include the East Siberian Sea Slope and Mendeleyev Ridge (Figure 1). Hereafter, the eastern area is referred to as the Chukchi marginal area (CMA), and the western area as the East Siberian marginal area (ESMA).

The migration of Pacific water (Codispoti et al., 2005; Woodgate et al., 2005) follows three pathways: the Alaskan coastal current, Bering shelf water, and Anadyr water (Woodgate et al., 2005). The CMA is influenced by the inflow of Anadyr water. Recent major oceanic changes in the study area include surface warming and sea ice retreat (Steele et al., 2008). For example, the mean ice edge retreat in September was much larger in 2007 than in previous years, and the maximum temperature anomaly in the northern Chukchi Sea in 2007 was double that of 2005, when a value of 2.5 °C was recorded. In the study area, chlorophyll-*a* (Chl-*a*) concentrations at the surface are remarkably low during summer and reflect nutrient depletion at the surface due to biological uptake and the intense stratification caused by large freshwater inputs (Carmack et al., 2006; Codispoti et al., 2005).

2.2. Methods

Hydrographic surveys were carried out from the IBRV *Araon* at 78 stations in the western Arctic Ocean, covering the Northwind Ridge, Chukchi Plateau, Chukchi Abyssal Plain, Chukchi Sea Slope, East Siberian Sea Slope, and Mendeleyev Ridge, during consecutive summers (August) in 2016–2018 (Figure 1). Surface temperature and salinity were measured using a calibrated conductivity-temperature-depth/pressure (CTD) recorder (SBE 911; Sea-Bird Electronics Inc., Bellevue, WA, USA). Seawater samples were collected for the measurement of dissolved inorganic carbon (DIC), total alkalinity (TA), and Chl-*a* using a Rosette sampler with 10-L Niskin bottles mounted on the CTD assembly.

Water samples for DIC and TA measurements were collected on board in 500-mL borosilicate glass bottles, with 200 μL of saturated $HgCl_2$ solution added to prevent biological alterations. DIC concentrations were measured using the VINDTA 3D system (Marianda, Kiel, Germany) coupled to a CO_2 coulometric titrator (Model 5011; UIC, Inc., Joliet, IL, USA), and TA concentrations using a potentiometric titration system (AS-ALK2; Apollo SciTech, Newark, DE, USA). Measurement uncertainty was evaluated on a daily basis using certified seawater reference materials provided by the Scripps Institute of Oceanography (University of California, San Diego, CA, USA). The precision of the DIC and TA measurements was within ±1.5 and ±2 $\mu mol\ kg^{-1}$, respectively. Water samples for Chl-*a* analysis were filtered through GF/F filters (47-mm, Whatman). The filtrate was then mixed with 90% acetone and allowed to stand for 24 h before the Chl-*a* concentration was determined shipboard using a fluorometer (Trilogy; Turner Designs, USA) that had been previously calibrated against pure Chl-*a* (Sigma, USA).

Seawater pH (total scale) and Ω_{arag} was calculated from the DIC, TA, temperature, salinity, phosphate, and silicate data using the CO2SYS program (Pierrot et al., 2006), with the constants of Mehrbach et al. (1973) and refit by Dickson and Millero (1987) for K_1 and K_2. The bisulfate dissociation constant was used from Dickson (1990), and the ratio of boron to chlorinity was taken from K. Lee et al. (2000). Calcium concentrations were determined from the salinity. The solubility product (K_{sp}) of aragonite was determined according to Mucci (1983). Dissolved organic acids may introduce an error in calculating the Ω_{arag} from DIC and TA, as they proportionally changed the contribution of other species (CO_3^{2-} and $B(OH)_4^-$) to TA (Ko et al., 2016). On the basis of the uncertainties of DIC and TA measurements and the thermodynamic constants, the Ω_{arag} uncertainty was estimated to be approximately 8%. Seawater aragonite supersaturation was defined as $\Omega_{arag} > 1.0$, and undersaturation as $\Omega_{arag} < 1.0$.

In the study area, surface water was a mixture of Atlantic water (ATW), meteoric water (MW), and sea ice meltwater (SIM) (Yamamoto-Kawai et al., 2005). Based on the relationship between the constant TA values for salinity, the fractions of each end-member can be calculated from the salinity and TA data using mass balance equations as follows:

$$f_{\mathrm{ATW}} + f_{\mathrm{MW}} + f_{\mathrm{SIM}} = 1$$

$$f_{\mathrm{ATW}} S_{\mathrm{ATM}} + f_{\mathrm{MW}} S_{\mathrm{MW}} + f_{\mathrm{SIM}} S_{\mathrm{SIM}} = S$$

$$f_{\mathrm{ATW}} \mathrm{TA}_{\mathrm{ATM}} + f_{\mathrm{MW}} \mathrm{TA}_{\mathrm{MW}} + f_{\mathrm{SIM}} \mathrm{TA}_{\mathrm{SIM}} = \mathrm{TA}$$

where f, S, and TA refer to the fraction, salinity, and total alkalinity, respectively. End-member values for salinity and TA were obtained from the data set of Yamamoto-Kawai et al. (2005); $S_{\mathrm{ATW}} = 34.87$, $S_{\mathrm{MW}} = 4.0$, $S_{\mathrm{SIM}} = 0$, $\mathrm{TA}_{\mathrm{ATW}} = 2306$ μmol kg^{-1}, $\mathrm{TA}_{\mathrm{MW}} = 263$ μmol kg^{-1}, and $\mathrm{TA}_{\mathrm{SIM}} = 831$ μmol kg^{-1}.

3. Results

The summertime sea ice concentration in the study area between 2016 and 2018 exhibited distinct spatio-temporal variations (Figure 2). During the study period, sea ice coverage was greater in the ESMA than in the CMA. Specifically, sea ice covered most of the ESMA in 2016 and 2018 and all of the ESMA in 2017 (Figure 2). In contrast, more than half of the sea ice in the CMA melted between 2016 and 2018 (Figure 2). Spatio-temporal variations in the sea ice distribution are expected to have significant effects on the physical and chemical characteristics of the surface water.

SST and sea surface salinity (SSS) were intimately associated with sea ice coverage (Figure 2). In the ESMA, with its extensive sea ice cover in summer, the surface water was colder and more saline than in the CMA (Table 1). The annual changes in SST and SSS were more pronounced in the CMA than in the ESMA (Table 1). In 2017, when almost all of the ESMA was covered with sea ice, the SST in those waters was lower than in 2016 and 2018, but the SSS was higher (Table 1).

The fraction of Atlantic water (f_{ATW}) from 2016 to 2018 ranged from 0.76 to 0.89, with an average of 0.82 (Figure 2). The fractions of meteoric water (f_{MW}) and sea ice meltwater (f_{SIM}) varied from 0.10 to 0.22 and from −0.04 to 0.05, respectively (Figure 2). The f_{ATW} was consistently higher in the ESMA than in the CMA, but the f_{MW} and f_{SIM} were consistently higher in the CMA than in the ESMA (Table 1).

Surface TA concentrations ranged from 1,922 to 21,36 μmol kg^{-1} during all 3 years, with higher values in the ESMA than in the CMA (Figure 3). In the latter, the distribution was similar to that of SSS. The surface TA distribution exhibited little annual variation from 2016 to 2018. Surface DIC concentrations ranged from 1,845 to 2,022 μmol kg^{-1} and resembled the distribution of TA (Figure 3). SSS was probably the main factor influencing the surface distribution of TA and DIC. The lower concentrations of TA and DIC in the CMA were likely due to the dilution of its waters with SIM.

Surface pH (total scale) varied from 7.98 to 8.37 during all three years, with higher values in the ESMA than in the CMA (Figure 3). In 2017, however, lower surface pH was observed in the ESMA (Figure 3). Surface Ω_{arag} ranged from 0.90 to 2.09 between 2016 and 2018, with higher values in the ESMA than in the CMA in 2016 and 2018 (Figure 3). In 2017, low surface Ω_{arag} values were measured in both areas (Figure 3). Aragonite undersaturation ($\Omega_{\mathrm{arag}} < 1.0$) at the surface waters was determined annually only in the CMA: at 2 stations in 2016, 1 station in 2017, and 5 stations in 2018.

4. Discussion

4.1. Regional Difference in the Carbonate Chemistry of Surface Water

The most distinctive feature of the study area was the difference in the seawater variables related to ocean acidification between the ESMA and CMA. Throughout the study, the surface water of the ESMA was always colder and more saline than that of the CMA (Table 1), as the latter received inflows of warmer, less saline water from the Pacific (Woodgate et al., 2005). The consistently higher surface TA and DIC concentrations in the ESMA than in the CMA (Table 2) reflected the lower SSS in the CMA. The surface Ω_{arag}

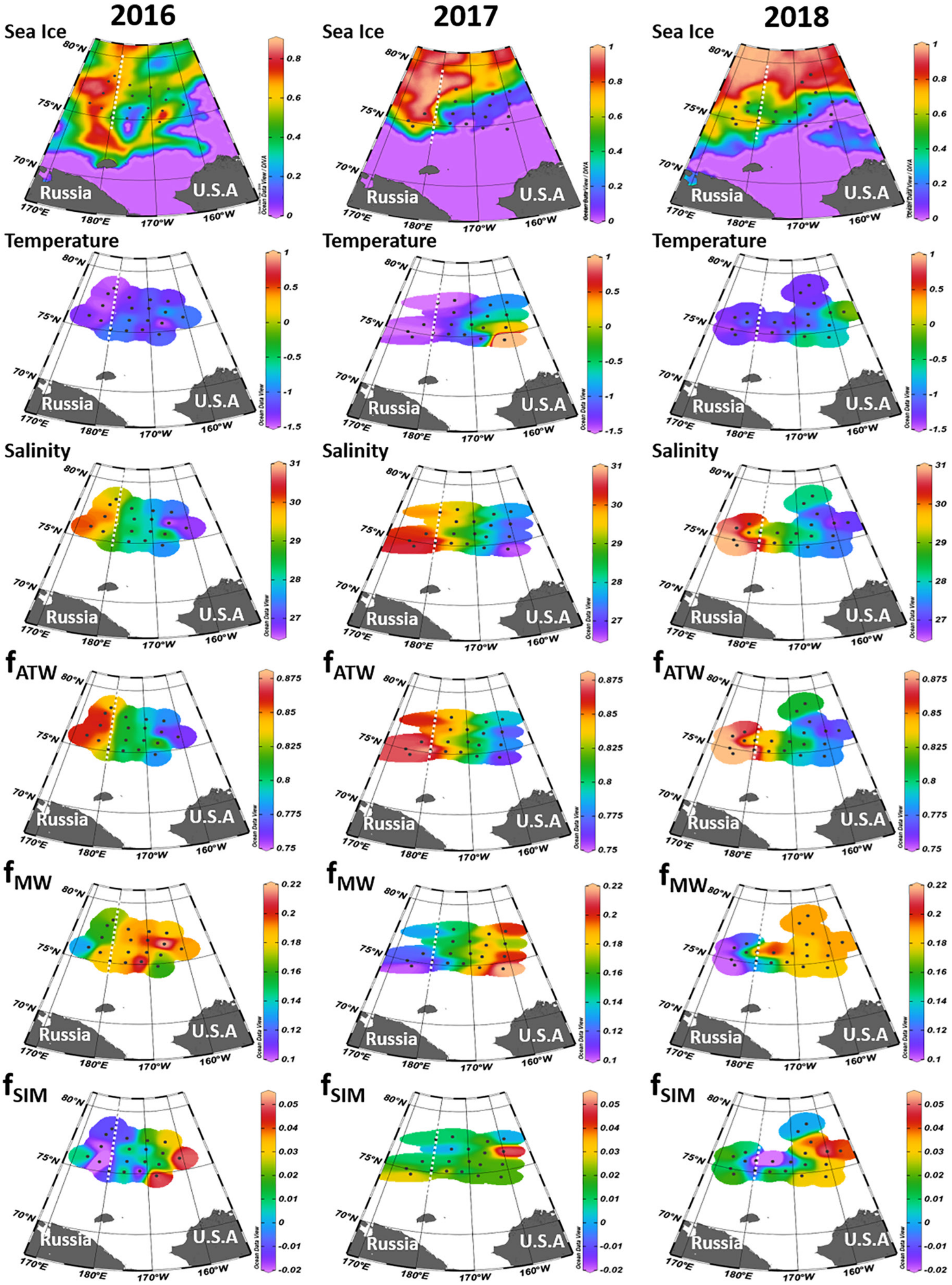

Figure 2. Surface distribution of sea ice, temperature, salinity, the Atlantic water fraction (f_{ATW}), the meteoric water fraction (f_{MW}), and the sea ice melt fraction (f_{SIM}) from 2016 to 2018. The white dotted line indicates the boundary between the Chukchi marginal area and the East Siberian marginal area.

Table 1

Average and One Standard Deviation Values of the Sea Surface Temperature (SST), Sea Surface Salinity (SSS), Atlantic Water Fraction (f_{ATW}), Meteoric Water Fraction (f_{MW}), and Sea Ice Melt Fraction (f_{SIM}) in the Chukchi Marginal Area (CMA) and East Siberian Marginal Area (ESMA) From 2016 to 2018

	SST (°C)		SSS		f_{ATW}		f_{MW}		f_{SIM}	
Year	CMA	ESMA	CMA	ESMA	CMA	ESMA	CMA	ESMA	CMA	ESMA
2016	−1.15 ± 0.18	−1.35 ± 0.18	27.8 ± 0.6	29.6 ± 0.5	0.80 ± 0.02	0.85 ± 0.01	0.19 ± 0.015	0.16 ± 0.02	0.014 ± 0.02	−0.014 ± 0.014
2017	−0.68 ± 0.93	−1.53 ± 0.074	28.3 ± 0.9	30.3 ± 0.3	0.81 ± 0.03	0.87 ± 0.007	0.17 ± 0.02	0.12 ± 0.01	0.018 ± 0.012	0.015 ± 0.006
2018	−0.92 ± 0.40	−1.30 ± 0.15	27.8 ± 0.7	30.2 ± 0.8	0.79 ± 0.02	0.87 ± 0.02	0.19 ± 0.01	0.13 ± 0.03	0.018 ± 0.025	0.004 ± 0.019

was higher in the ESMA than in the CMA in 2016 and 2018, but lower in the ESMA in 2017 (Table 2). The difference in the surface Ω_{arag} between the CMA and ESMA may have been due to the different processes affecting the Ω_{arag} in these two areas.

In the CMA, SSS correlated well with DIC and TA (Figure 4), indicating that the DIC and TA concentrations were determined mainly by the mixing of seawater with the freshwater introduced from rivers and/or sea ice (Robbins et al., 2013; Yamamoto-Kawai et al., 2009). The good correlation of the surface Ω_{arag} with SSS in the CMA during the three years of the study (Figure 4) suggested that Ω_{arag} was controlled mainly by freshwater dilutions. Of the two sources of freshwater, MW and SIM (Yamamoto-Kawai et al., 2005), f_{SIM} correlated negatively with surface Ω_{arag} in 2016, 2017, and 2018 (Figure 5), whereas the correlation of f_{MW} was moderate and occurred only in 2017 (Figure 5). The strong negative correlation between f_{SIM} and the surface Ω_{arag} in the CMA was due to the strong dilution with SIM that influenced the surface Ω_{arag}. This result was consistent with a previous study of the adjacent Canada Basin, which showed that the main mechanism controlling Ω_{arag} was dilution with SIM (Robbins et al., 2013).

In the ESMA, TA correlated well with SSS during all research periods, but DIC was only well correlated with SSS in 2017 (Figure 6). Surface Ω_{arag} and SSS were only well correlated in 2016 (Figure 6). Neither of the freshwater sources were correlated with surface Ω_{arag} at any time during the study (data not shown). Therefore, the spatial variation in seawater carbonate chemistry in the ESMA was not solely due to dilution with SIM; rather, physical and biological processes likely also influenced the changes in seawater carbonate chemistry associated with ocean acidification in the surface waters of the ESMA (Chierici & Fransson, 2009). These processes are discussed in detail in the following sections.

4.2. Annual Variations in the Surface Water Carbonate Chemistry

Annual changes in seawater carbonate chemistry differed between the CMA and ESMA. In the CMA, there was no significant annual variation in the surface Ω_{arag} or the SST, SSS, DIC, or TA from 2016 to 2018 (Figure 3). In contrast, in the ESMA the surface Ω_{arag} underwent very large annual changes during the 3 years of the study and was highest (average of 1.86) in 2018 and lowest (1.18) in 2017 (Table 2). Although no significant annual changes were observed in the TA, relatively large annual changes were observed in the DIC (Table 2).

As noted in the previous section, the strong correlation in the CMA of DIC with both SSS and f_{SIM} indicated that the DIC concentration was determined primarily by dilution with SIM, with little effect of the biological activity in surface water. Additionally, the nearly constant average DIC concentrations in the CMA measured throughout the study (Table 2) suggested that biological activity also did not change considerably during the same time period. Pacific water flowing through the Bering Strait flows through the Alaska coastal current to the Canada Basin or through the Chukchi Shelf to the CMA (Woodgate et al., 2005). During the summer, and thus in the absence of sea ice, annual primary productivity in the Chukchi Shelf was high (>300 gC m^{-2}), due to the inflow of nutrient-rich Pacific water (Bates & Mathis, 2009). However, nutrient exhaustion within the Chukchi Shelf resulted in the inflow of nutrient-poor water into the CMA, such that biological production in those waters was low (S. H. Lee et al., 2012; Yun et al., 2015). The relatively low depth-integrated Chl-*a* concentrations in the CMA (Table 2) were consistent with the low biological activity in this region, and their lack of significant annual variation (Table 2) suggested that the inflow of nutrient-poor shelf water did not change considerably during the study period.

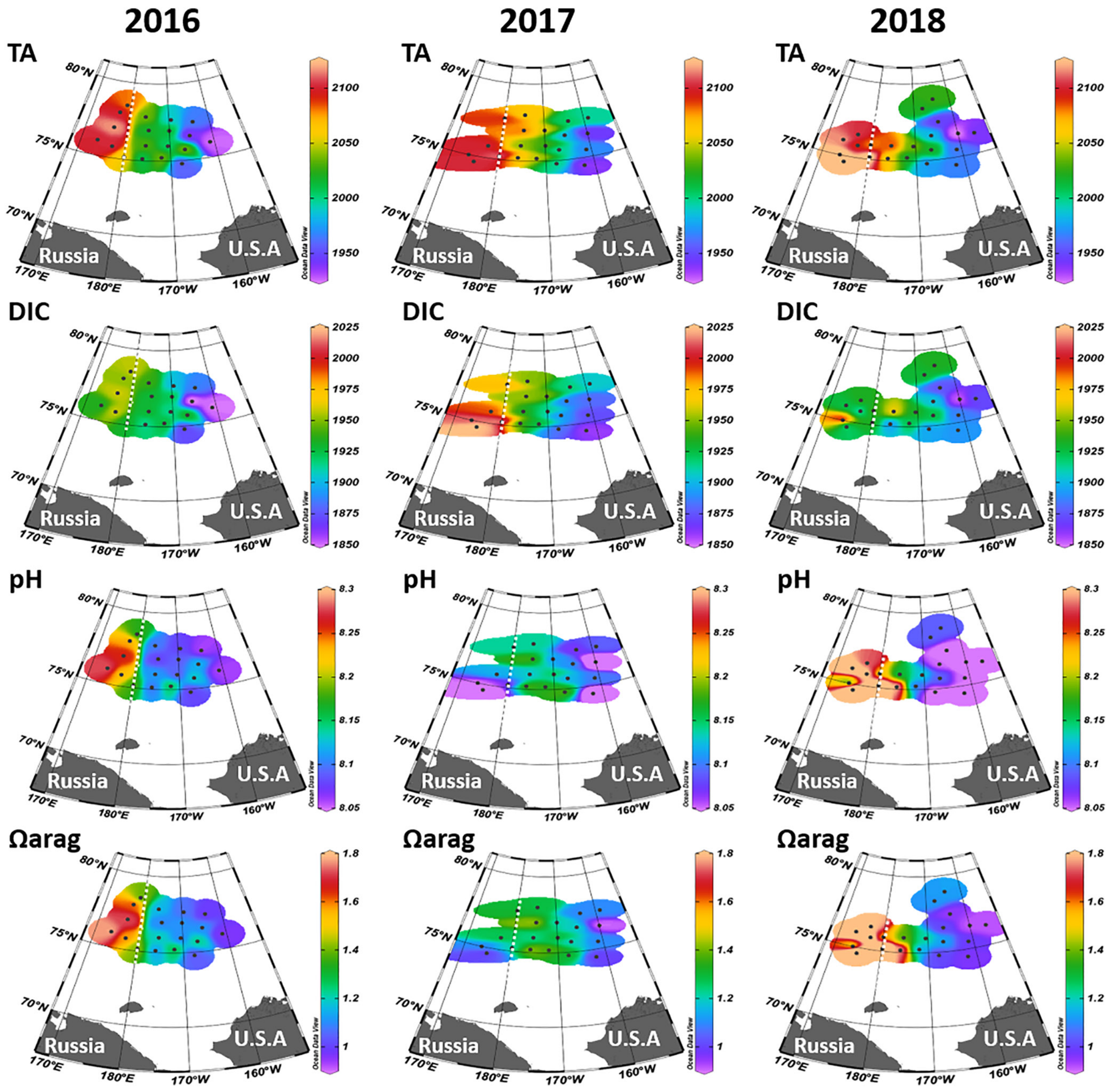

Figure 3. Surface distribution of total alkalinity, dissolved inorganic carbon, pH (total scale), and the aragonite saturation state from 2016 to 2018. The white dotted line indicates the boundary between the Chukchi marginal area and the East Siberian marginal area.

Unlike the CMA, DIC concentrations in the ESMA did not correlate well with SSS in the summers of 2016 and 2018, but a correlation was observed in 2017 (Figure 6). This pattern suggests that DIC concentrations are affected by processes other than dilution with freshwater, such as biological activity, sea-air CO_2 exchange, and vertical/lateral mixing (Chierici & Fransson, 2009). The average DIC concentration in the ESMA changed significantly over the 3 years, with the highest value in 2017 and the lowest value in 2018 (Table 2). This result suggests differences in the processes annually affecting the DIC concentration or in their extent. In 2016 and 2018, DIC concentrations in the CMA were lower than the linear mixing line with SSS (Figure 6), indicating that biological activity exerted strong effects at the sea surface and constituted the main mechanism leading to a reduction in the DIC concentration (Bates et al., 2013; Chierici & Fransson, 2009). In 2017, DIC concentrations were higher than the linear mixing line with SSS (Figure 6),

Table 2
Average and One Standard Deviation Values of the Total Alkalinity (TA), Dissolved Inorganic Carbon (DIC), pH, Aragonite Saturation State (Ω_{arag}), and Depth-Integrated Chlorophyll-a (DChl-a) in Chukchi Marginal Area (CMA) and East Siberian Marginal Area (ESMA) From 2016 to 2018

	TA (μmol kg^{-1})		DIC (μmol kg^{-1})		pH (total scale)		Ω_{arag}		DChl-*a* (mg m^{-2})	
Year	CMA	ESMA	CMA	ESMA	CMA	ESMA	CMA	ESMA	CMA	ESMA
2016	1,997 ± 39	2,093 ± 21	1,905 ± 32	1,949 ± 13	8.10 ± 0.03	8.23 ± 0.04	1.11 ± 0.09	1.59 ± 0.16	16.5 ± 12	32.9 ± 8.5
2017	2,014 ± 44	2,102 ± 9.2	1,910 ± 30	2,006 ± 22	8.12 ± 0.06	8.07 ± 0.06	1.21 ± 0.15	1.18 ± 0.13	12.8 ± 5.4	22.7 ± 24
2018	1,993 ± 46	2,107 ± 28	1,907 ± 31	1,932 ± 32	8.11 ± 0.10	8.28 ± 0.07	1.07 ± 0.14	1.86 ± 0.26	17.5 ± 18	94.7 ± 3.5

indicating a less prominent role for biological activity. The Chl-*a* concentration followed a trend opposite that of the DIC concentration, as the average depth-integrated Chl-*a* concentration was highest (94.7 mg m^{-2}) in 2018, when the DIC concentration was the lowest, and lowest (22.7 mg m^{-2}) in 2017, when the DIC concentration was the highest (Table 2). Thus, the annual variation in the DIC concentration was closely related to biological activity in the surface layer.

In general, Ω_{arag} was mainly determined by the DIC and TA concentrations (Bates et al., 2009; Chierici & Fransson, 2009). In the ESMA, the large annual variation in the surface Ω_{arag} could be attributed to the annual change in the DIC concentration associated with biological activity in the surface layer, because TA

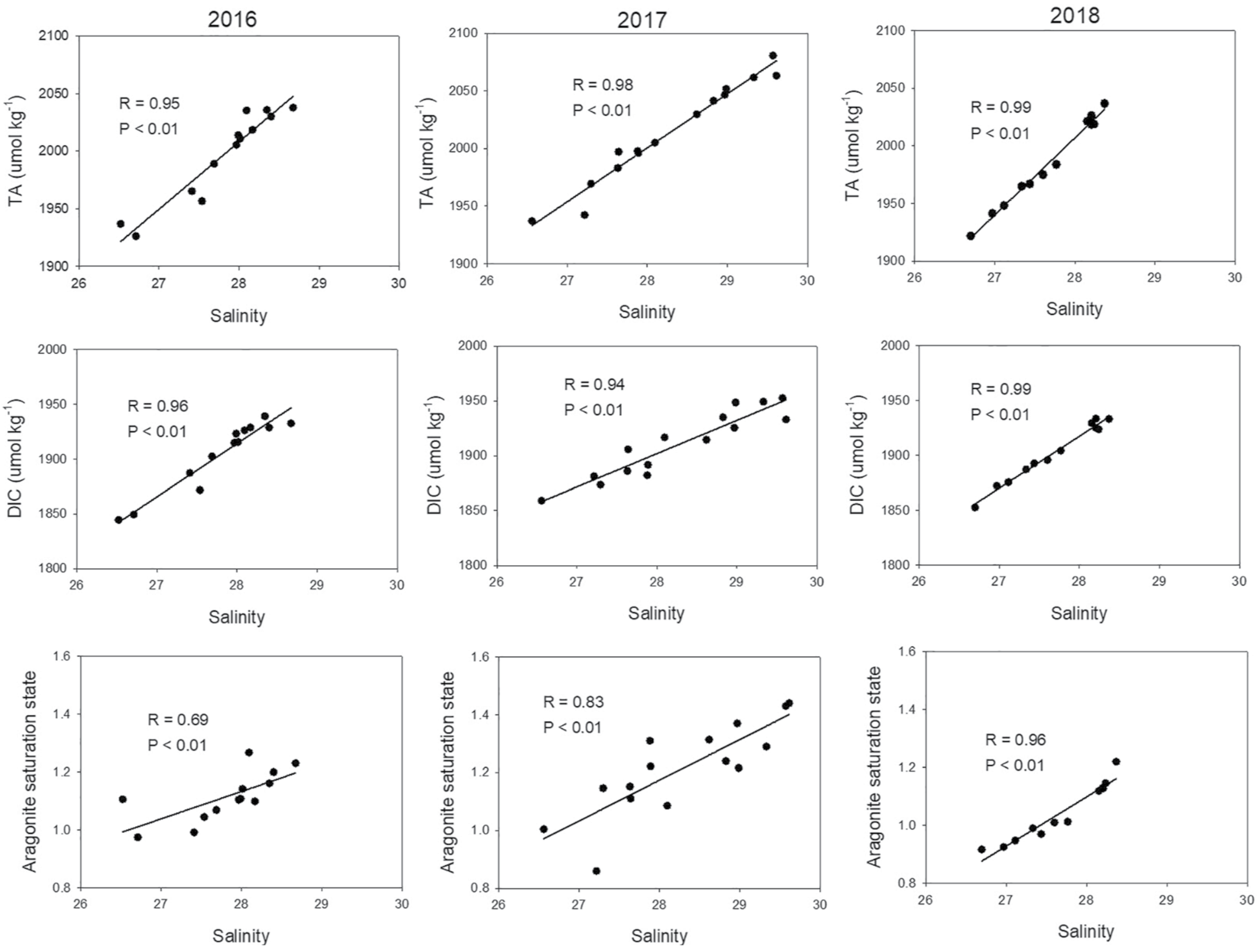

Figure 4. Salinity versus total alkalinity, dissolved inorganic carbon, and the aragonite saturation state in the Chukchi marginal area from 2016 to 2018. Solid lines represent linear regression lines.

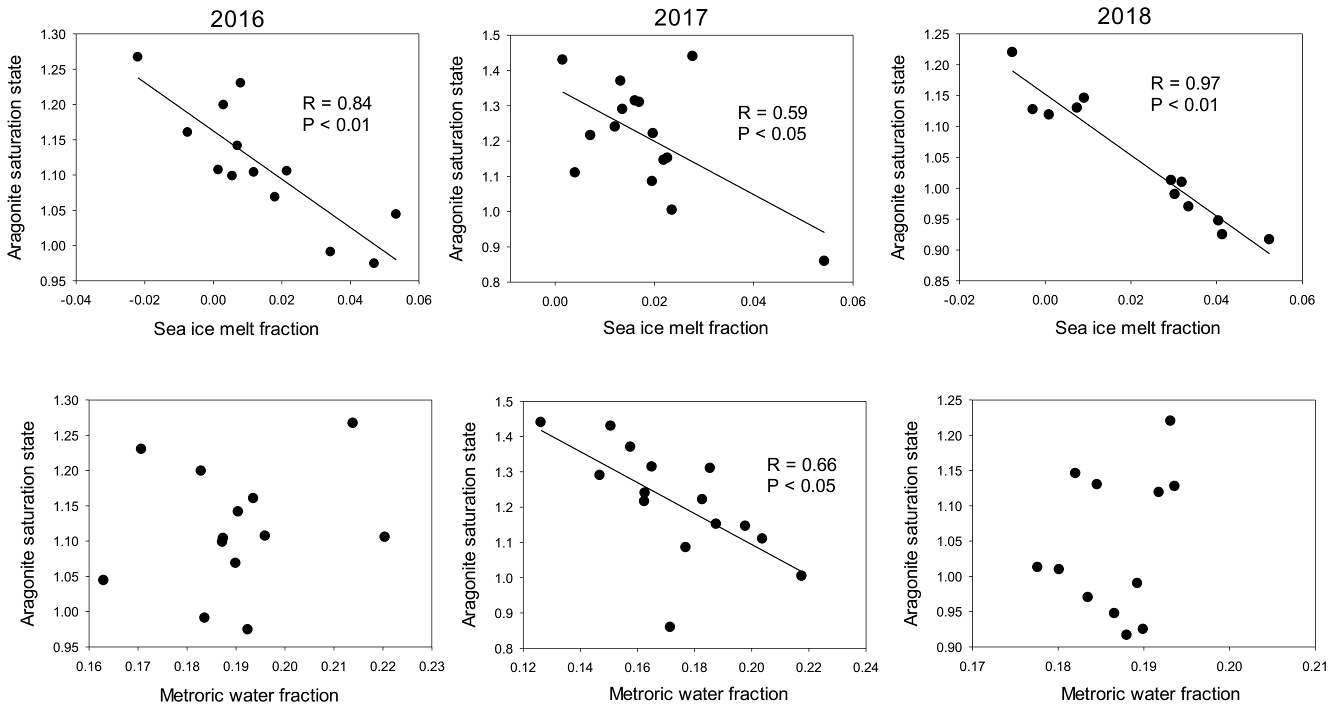

Figure 5. Aragonite saturation state versus the sea ice melt fraction and meteoric water fraction in the Chukchi marginal area from 2016 to 2018. Solid lines represent linear regression lines.

did not exhibit a significant annual variation. In 2016 and 2018, the surface Ω_{arag} was considerably higher in the ESMA than in the CMA (Table 2), due to the high biological production in the former in both years, However, the surface Ω_{arag} in the ESMA was much lower in 2017 than in 2016 and 2018, and even lower than in the CMA in 2017 (Table 2). In contrast, DIC concentration was fairly higher in 2017 than those in 2016 and 2018, and thereby, the lower surface Ω_{arag} was ascribed to the higher DIC concentration in 2017 since the higher DIC relative TA reduced CO_3^{2-} and as a result, lowered Ω_{arag} (Bates et al., 2009; Chierici & Fransson, 2009). In 2017, DIC concentrations higher than the linear mixing line with SSS (Figure 6) pointed to additional processes, such as vertical/lateral mixing with DIC-enriched waters and/or the influx of atmospheric CO_2 (Chierici & Fransson, 2009). Since about 90% of the ESMA area was covered by sea ice in 2017 (Figure 2), an influx of atmospheric CO_2 was ruled out as the DIC-adding process. Therefore, the main process for the DIC increment beyond that resulting from the mixing of seawater and freshwater in 2017 was vertical/lateral mixing with DIC-enriched waters.

Anderson et al. (2017) reported that nutrient-rich water was exported from the shelf to the deep basin in the East Siberian Sea. This may have had a considerable influence on the seawater carbonate chemistry in the ESMA because the inflow of nutrient-rich shelf water may have increased primary production in the ESMA, as suggested by depth-integrated Chl-*a* concentrations 2.1 and 4.5 times higher in the ESMA than in the CMA in 2016 and 2018, respectively (Table 2). In both years, the higher surface Ω_{arag} could be attributed to the lower DIC concentrations resulting from the increased biological production. However, the relatively low surface Ω_{arag} in 2017 reflected the higher DIC concentrations derived from the lateral mixing with DIC-enriched waters and less biological uptake of DIC. The inflow of the nutrient- and DIC-rich shelf water in 2017 would have enhanced surface DIC concentrations (Semiletov et al., 2016). In August 2017, when sea ice covered almost all of the surface water (Figure 2), biological production would have been accordingly depressed, such that there would have been no significant consumption of DIC.

4.3. Comparison With Shelf Areas

In the Chukchi Shelf, surface Ω_{arag} values were typically >1.0 (Bates et al., 2013; Chierici & Fransson, 2009) indicated aragonite oversaturation, with values generally higher than those in the CMA. The higher surface

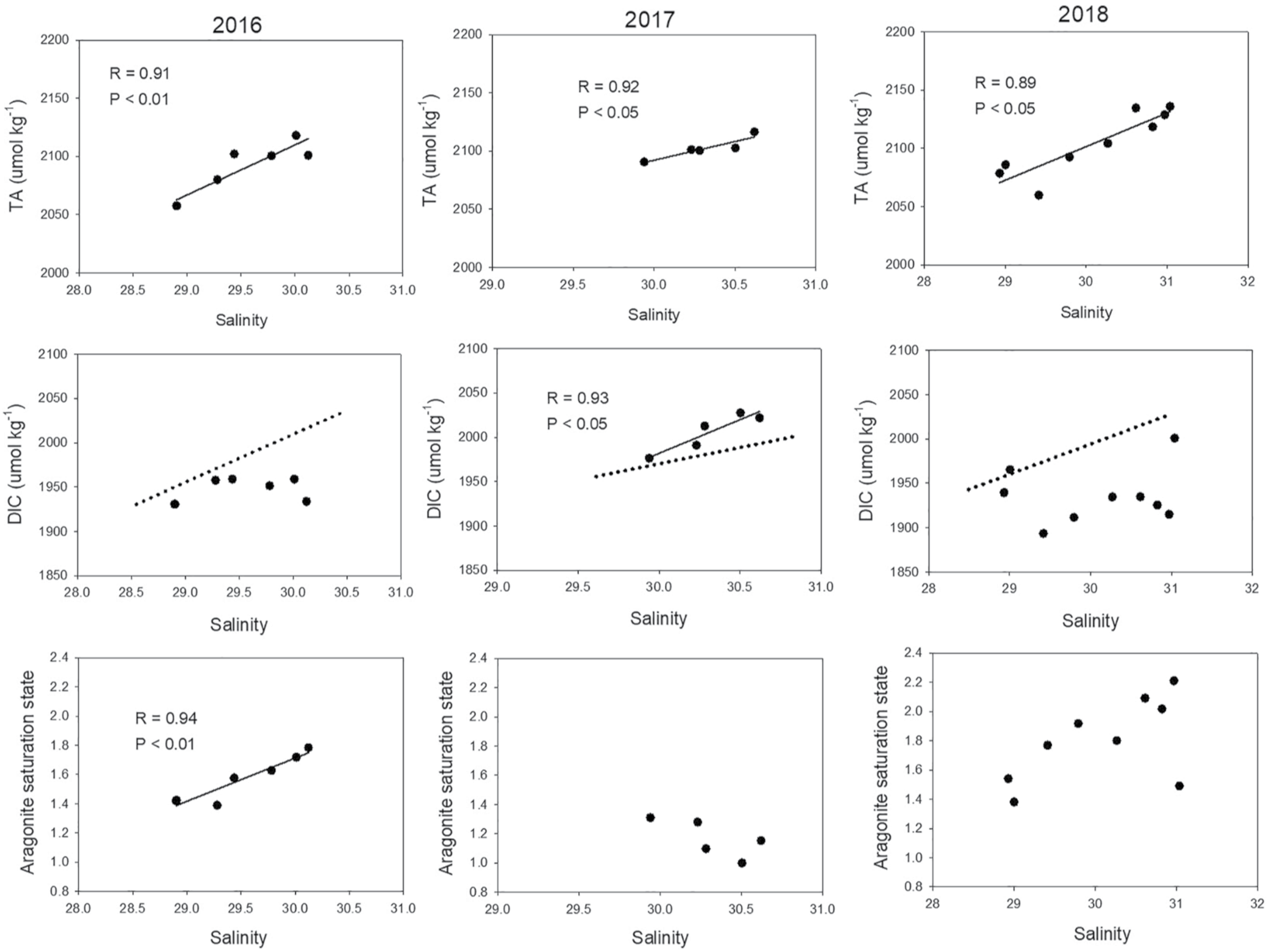

Figure 6. Salinity versus total alkalinity, dissolved inorganic carbon (DIC), and the aragonite saturation state in the East Siberian marginal area from 2016 to 2018. Solid lines represent linear regression lines, and dotted lines represent linear mixing lines of DIC versus salinity in the Chukchi marginal area.

Ω_{arag} in the Chukchi Shelf could be explained by the high primary production derived from the inflow of nutrition-rich Pacific waters (Bates & Mathis, 2009; Bates et al., 2013). High primary production reduces $p\mathrm{CO}_2$ and DIC concentrations, eventually increasing Ω_{arag}. Unlike in the Chukchi Shelf, primary production in the CMA was relatively low, as the nutrient supply was not sufficient to sustain a high level of production (S. H. Lee et al., 2012; Yun et al., 2015). As a result, TA and DIC concentrations were mainly affected by the dilution with freshwater in the CMA and thereby, surface Ω_{arag} was also determined by the dilution with freshwater. In the CMA, surface Ω_{arag} ranged from 0.86 to 1.77 between 2016 and 2018. The average value of 1.16 indicated near saturation with aragonite. Aragonite undersaturation was determined at only 2 (14%) stations in 2016, 1 station in (7%) in 2017, and 5 stations (36%) in 2018, similar to the report that ~20% of the surface waters in the Canada Basin, where the surface water is directly affected by Pacific waters, were undersaturated with aragonite (Robins et al., 2013). However, in contrast to the warmer, less saline surface waters (<25) of the Canada Basin (Robins et al., 2013), the SSS in the CMA was generally >26, which indicated less oceanic acidification than in the Canada Basin.

In the East Siberian Shelf, the surface Ω_{arag} was generally <1.0 (Semiletov et al., 2016), consistent with aragonite undersaturation, whereas in the Chukchi Shelf oversaturation was observed. The aragonite undersaturation in the East Siberian Shelf was mainly due to the degradation of terrestrial organic matter and the discharge of Arctic river water with a high $p\mathrm{CO}_2$ (Semiletov et al., 2016). The introduction of terrestrial organic matter and high-$p\mathrm{CO}_2$ river water into the East Siberian Shelf increased the $p\mathrm{CO}_2$ of the shelf water and reduced the surface Ω_{arag} to <1. In the ESMA, the surface Ω_{arag} ranged from 1.01 to 2.21 between 2016 and 2018, with a higher average (1.59) than in the East Siberian Shelf (Semiletov et al., 2016). Additionally, the absence of aragonite undersaturation in the ESMA during the study period indicated that ocean acidification was less seriously progressing in the ESMA than in the East Siberian Shelf. The higher surface Ω_{arag} in the ESMA was mainly ascribed to high primary production, evidenced by the relatively high depth-integrated Chl-*a* concentration in this area (Table 2). The inflows of nutrient-rich shelf water in 2016 and 2018 would have increased primary production in the ESMA. In 2017, the surface Ω_{arag} was much lower than in 2016 and 2018, and even lower than in the CMA in 2017. This lower surface Ω_{arag} in 2017 is best explained by the intrusion of DIC-enriched shelf water and the extensive sea ice cover, which depressed biological production at the surface.

5. Conclusions

The study area was divided along a longitude of 108°E into the CMA and ESMA, with water depths ranging from 90 to 2,200 m. The CMA is influenced by the inflow of Pacific water, which results in warmer, less saline surface waters, whereas in the ESMA inflows of nutrient-enriched shelf water lead to high-level biological production. We found that in the CMA and the ESMA, the surface Ω_{arag} was determined mainly by the mixing of seawater and freshwater introduced from rivers and/or sea ice; however, in the ESMA, additional processes of biological production and lateral mixing were also involved. The surface Ω_{arag} was higher in the ESMA than in the CMA in 2016 and 2018, but lower in the ESMA in 2017. Between 2016 and 2018, the surface Ω_{arag} in the CMA did not undergo significant annual variation, unlike in the ESMA, where large annual changes were due to the large annual variation in the surface DIC concentrations. The inflow of nutrient-enriched shelf water in the ESMA stimulated biological production in 2016 and 2018, thus reducing DIC concentrations. In 2017, the relatively high DIC concentrations were explained by the extensive sea ice cover, which depressed biological production.

In the CMA, surface Ω_{arag} ranged from 0.86 to 1.77 from 2016 to 2018, with an average value of 1.16, close to Ω_{arag}. Aragonite undersaturation was detected at only 2 stations (14%) in 2016, 1 station (7%) in 2017, and 5 stations (36%) in 2018, consistent with a previous report that ~20% of the surface waters of the Canada Basin, which is directly affected by Pacific waters, were undersaturated with respect to aragonite. Although the SSS (<25) in the Canada Basin was extremely low, this was not the case in the CMA. According to these results, oceanic acidification is less serious in the CMA than in the Canada Basin. In the ESMA, the surface Ω_{arag} ranged from 1.01 to 2.21 between 2016 and 2018, with an average value (1.59) higher than that determined for the CMA. Aragonite undersaturation in the ESMA was not observed during any of the measurement periods, so ocean acidification was less serious there than in the CMA. The higher surface Ω_{arag} in the ESMA is mainly explained by the high level of primary production, as evidenced by the relatively high depth-integrated Chl-*a* concentration in this area.

Ocean acidification, and thus decreases in the surface Ω_{arag}, can be expected to progress in the CMA, because freshwater inputs from sea ice melts will continue to increase in the foreseeable future. The undersaturation of aragonite in the CMA threatens the existence of calcareous organisms and may lead to their extinction. However, a similar scenario in the ESMA in the near future is unlikely, because the relatively high biological production characteristic of its waters results in a high surface Ω_{arag} such that aragonite undersaturation of the surface water is avoided. Monitoring ocean acidification in the western Arctic Ocean will require more research focusing on the carbonate chemistry in these waters.

Data Availability Statement

The data for this work are available at https://www.ncei.noaa.gov/data/oceans/ncei/ocads/metadata/0241111.html.

Acknowledgment

This work was supported by project PE99912 of the Korea Institute of Ocean Science and Technology, and in part by the project titled "Korea-Arctic Ocean Warming and Response of Ecosystem (K-AWARE, KOPRI, 1525011760)," funded by the Ministry of Oceans and Fisheries, Korea.

References

Anderson, L. G., Bjork, G., Holby, O., Jutterstrom, S., Morth, C. M., O'Regan, M., et al. (2017). Shelf-basin interaction along the East Siberian Sea. *Ocean Science*, *13*(2), 349–363. https://doi.org/10.5194/os-13-349-2017

Bai, Y. C., Sicre, M. A., Chen, J. F., Klein, V., Jin, H. Y., Ren, J., et al. (2019). Seasonal and spatial variability of sea ice and phytoplankton biomarker flux in the Chukchi Sea (western Arctic Ocean). *Progress in Oceanography*, *171*, 22–37. https://doi.org/10.1016/j.pocean.2018.12.002

Bates, N. R., & Mathis, J. T. (2009). The Arctic Ocean marine carbon cycle: Evaluation of air-sea CO_2 exchanges, ocean acidification impacts and potential feedbacks. *Biogeosciences*, *6*(11), 2433–2459. https://doi.org/10.5194/bg-6-2433-2009

Bates, N. R., Mathis, J. T., & Cooper, L. W. (2009). Ocean acidification and biologically induced seasonality of carbonate mineral saturation states in the western Arctic Ocean. *Journal of Geophysical Research*, *114*, 21. https://doi.org/10.1029/2008jc004862

Bates, N. R., Moran, S. B., Hansell, D. A., & Mathis, J. T. (2006). An increasing CO_2 sink in the Arctic Ocean due to sea-ice loss. *Geophysical Research Letters*, *33*(23). https://doi.org/10.1029/2006gl027028

Bates, N. R., Orchowska, M. I., Garley, R., & Mathis, J. T. (2013). Summertime calcium carbonate undersaturation in shelf waters of the western Arctic Ocean—How biological processes exacerbate the impact of ocean acidification. *Biogeosciences*, *10*(8), 5281–5309. https://doi.org/10.5194/bg-10-5281-2013

Carmack, E., Barber, D., Christensen, J., Macdonald, R., Rudels, B., & Sakshaug, E. (2006). Climate variability and physical forcing of the food webs and the carbon budget on panarctic shelves. *Progress in Oceanography*, *71*(2–4), 145–181. https://doi.org/10.1016/j.pocean.2006.10.005

Chierici, M., & Fransson, A. (2009). Calcium carbonate saturation in the surface water of the Arctic Ocean: Undersaturation in freshwater influenced shelves. *Biogeosciences*, *6*(11), 2421–2431. https://doi.org/10.5194/bg-6-2421-2009

Codispoti, L. A., Flagg, C., Kelly, V., & Swift, J. H. (2005). Hydrographic conditions during the 2002 SBI process experiments. *Deep Sea Research Part II: Topical Studies in Oceanography*, *52*(24–26), 3199–3226. https://doi.org/10.1016/j.dsr2.2005.10.007

Comiso, J. C., Parkinson, C. L., Gersten, R., & Stock, L. (2008). Accelerated decline in the Arctic Sea ice cover. *Geophysical Research Letters*, *35*(1). https://doi.org/10.1029/2007gl031972

Cross, J. N., Mathis, J. T., Pickart, R. S., & Bates, N. R. (2018). Formation and transport of corrosive water in the Pacific Arctic region. *Deep Sea Research Part II: Topical Studies in Oceanography*, *152*, 67–81. https://doi.org/10.1016/j.dsr2.2018.05.020

Dickson, A. G. (1990). Standard potential of the reaction: $AgCl(s) + H_2(g) = Ag(s) + HCl(aq)$, and the standard acidity constant of the ion HSO_4^- in synthetic sea water from 273.15 to 318.15 K. *Journal of Chemical Thermodynamics*, *22*, 113–127. https://doi.org/10.1016/0021-9614(90)90074-Z

Dickson, A. G., & Millero, F. J. (1987). A comparison of the equilibrium-constants for the dissociation of carbonic-acid in seawater media. *Deep-Sea Research Part A: Oceanographic Research*, *34*(10), 1733–1743. https://doi.org/10.1016/0198-0149(87)90021-5

Gao, Z. Y., Chen, L. Q., Sun, H., Chen, B. S., & Cai, W. J. (2012). Distributions and air-sea fluxes of carbon dioxide in the Western Arctic Ocean. *Deep Sea Research Part II: Topical Studies in Oceanography*, *81–84*, 46–52. https://doi.org/10.1016/j.dsr2.2012.08.021

Ko, Y. H., Lee, K., Eom, K. H., & Han, I.-S. (2016). Organic alkalinity produced by phytoplankton and its effect on the computation of ocean carbon parameters. *Limnology & Oceanography*, *61*, 1462–1471. https://doi.org/10.1002/lno.10309

Lee, K., Kim, T.-W., Byrne, R. H., Millero, F. J., Feely, R. A., & Liu, Y.-M. (2000). The universal ratio of boron to chlorinity for the North Pacific and North Atlantic oceans. *Geochimica et Cosmochimica Acta*, *74*, 1801–1811. https://doi.org/10.1016/j.gca.2009.12.027

Lee, S. H., Joo, H. M., Liu, Z. L., Chen, J. F., & He, J. F. (2012). Phytoplankton productivity in newly opened waters of the Western Arctic Ocean. *Deep Sea Research Part II: Topical Studies in Oceanography*, *81–84*, 18–27. https://doi.org/10.1016/j.dsr2.2011.06.005

Mathis, J. T., & Questel, J. M. (2013). Assessing seasonal changes in carbonate parameters across small spatial gradients in the Northeastern Chukchi Sea. *Continental Shelf Research*, *67*, 42–51. https://doi.org/10.1016/j.csr.2013.04.041

Mehrbach, C., Culberson, C., Hawley, J., & Pytkowicx, R. (1973). Measurement of the apparent dissociation constants of carbonic acid in seawater at atmospheric pressure 1. *Limnology & Oceanography*, *18*(6), 897–907. https://doi.org/10.4319/lo.1973.18.6.0897

Mucci, A. (1983). The solubility of calcite and aragonite in seawater at various salinities, temperatures, and one atmosphere total pressure. *American Journal of Science*, *283*(7), 780–799. https://doi.org/10.2475/ajs.283.7.780

Orr, J. C., Fabry, V. J., Aumont, O., Bopp, L., Doney, S. C., Feely, R. A., et al. (2005). Anthropogenic ocean acidification over the twenty-first century and its impact on calcifying organisms. *Nature*, *437*(7059), 681–686. https://doi.org/10.1038/nature04095

Overland, J. E., & Wang, M. Y. (2013). When will the summer Arctic be nearly sea ice free? *Geophysical Research Letters*, *40*(10), 2097–2101. https://doi.org/10.1002/grl.50316

Pierrot, D., Lewis, E., & Wallace, D. (2006). *MS Excel program developed for CO_2 system calculations* (ORNL/CDIAC-105a). Carbon Dioxide Information Analysis Center, Oak Ridge National Laboratory, US Department of Energy.

Qi, D., Chen, L. Q., Chen, B. S., Gao, Z. Y., Zhong, W. L., Feely, R. A., et al. (2017). Increase in acidifying water in the western Arctic Ocean. *Nature Climate Change*, *7*(3), 195, 199-+. https://doi.org/10.1038/nclimate3228

Robbins, L. L., Wynn, J. G., Lisle, J. T., Yates, K. K., Knorr, P. O., Byrne, R. H., et al. (2013). Baseline monitoring of the western Arctic Ocean estimates 20% of Canadian basin surface waters are undersaturated with respect to aragonite. *PLoS One*, *8*(9), 15. https://doi.org/10.1371/journal.pone.0073796

Semiletov, I., Pipko, I., Gustafsson, O., Anderson, L. G., Sergienko, V., Pugach, S., et al. (2016). Acidification of East Siberian Arctic Shelf waters through addition of freshwater and terrestrial carbon. *Nature Geoscience*, *9*(5), 361–365. https://doi.org/10.1038/ngeo2695

Steele, M., Ermold, W., & Zhang, J. (2008). Arctic Ocean surface warming trends over the past 100 years. *Geophysical Research Letters*, *35*(2). https://doi.org/10.1029/2007GL031651

Steele, M., Zhang, J., & Ermold, W. (2010). Mechanisms of summertime upper Arctic Ocean warming and the effect on sea ice melt. *Journal of Geophysical Research*, *115*. https://doi.org/10.1029/2009jc005849

Steinacher, M., Joos, F., Frolicher, T. L., Plattner, G. K., & Doney, S. C. (2009). Imminent ocean acidification in the Arctic projected with the NCAR global coupled carbon cycle-climate model. *Biogeosciences*, *6*(4), 515–533. https://doi.org/10.5194/bg-6-515-2009

Timmermans, M. L., Proshutinsky, A., Krishfield, R. A., Perovich, D. K., Richter-Menge, J. A., Stanton, T. P., & Toole, J. M. (2011). Surface freshening in the Arctic Ocean's Eurasian Basin: An apparent consequence of recent change in the wind-driven circulation. *Journal of Geophysical Research*, *116*. https://doi.org/10.1029/2011jc006975

Woodgate, R. A., Aagaard, K., & Weingartner, T. J. (2005). A year in the physical oceanography of the Chukchi Sea: Moored measurements from autumn 1990-1991. *Deep Sea Research Part II: Topical Studies in Oceanography*, *52*(24–26), 3116–3149. https://doi.org/10.1016/j.dsr2.2005.10.016

Woodgate, R. A., Weingartner, T. J., & Lindsay, R. (2012). Observed increases in Bering Strait oceanic fluxes from the Pacific to the Arctic from 2001 to 2011 and their impacts on the Arctic Ocean water column. *Geophysical Research Letters*, *39*. https://doi.org/10.1029/2012gl054092

Yamamoto, A., Kawamiya, M., Ishida, A., Yamanaka, Y., & Watanabe, S. (2012). Impact of rapid sea-ice reduction in the Arctic Ocean on the rate of ocean acidification. *Biogeosciences*, *9*(6), 2365–2375. https://doi.org/10.5194/bg-9-2365-2012

Yamamoto-Kawai, M., McLaughlin, F. A., Carmack, E. C., Nishino, S., & Shimada, K. (2009). Aragonite undersaturation in the Arctic Ocean: Effects of ocean acidification and sea ice melt. *Science*, *326*(5956), 1098–1100. https://doi.org/10.1126/science.1174190

Yamamoto-Kawai, M., Mifune, T., Kikuchi, T., & Nishino, S. (2016). Seasonal variation of $CaCO_3$ saturation state in bottom water of a biological hotspot in the Chukchi Sea, Arctic Ocean. *Biogeosciences*, *13*(22), 6155–6169. https://doi.org/10.5194/bg-13-6155-2016

Yamamoto-Kawai, M., Tanaka, N., & Pivovarov, S. (2005). Freshwater and brine behaviors in the Arctic Ocean deduced from historical data of delta O-18 and alkalinity (1929-2002 AD). *Journal of Geophysical Research*, *110*(C10). https://doi.org/10.1029/2004jc002793

Yun, M. S., Kim, B. K., Joo, H. T., Yang, E. J., Nishino, S., Chung, K. H., et al. (2015). Regional productivity of phytoplankton in the Western Arctic Ocean during summer in 2010. *Deep Sea Research Part II: Topical Studies in Oceanography*, *120*, 61–71. https://doi.org/10.1016/j.dsr2.2014.11.023